# Supporting Information (to be published online) to the manuscript

## On the nature of the "dark S*" excited state of β-carotene

by Evgeny E. Ostroumov, Marc G. Müller, Michael Reus, and Alfred R. Holzwarth

Max-Planck-Institut für Bioanorganische Chemie, Stiftstr. 34-36, 45470 Mülheim a.d. Ruhr, Germany, Fax: +49 208 3063951, Tel.: +49 208 3063571

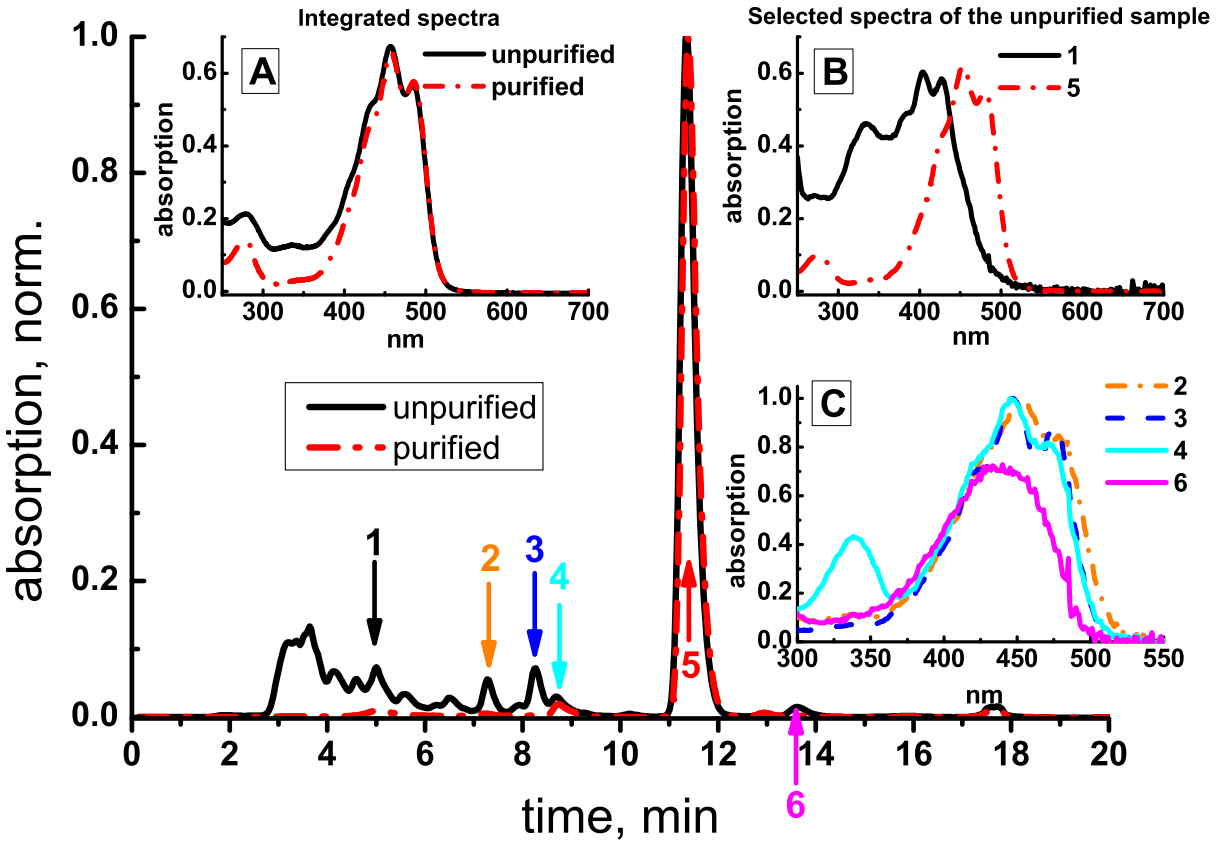


Figure S1. HPLC profiles of β-carotene in MTHF before (black solid lines) and after (red dash-dotted lines) purification, extraction wavelength 400 nm. Corresponding absorption spectra (in MTHF) are shown in inset A. The absorption spectra of elution peaks taken after 5 and 11.3 minutes (as indicated by arrows) shown in inset B were recorded directly on the diode array in the ethanol:methanol:tetrahydrofuran mixture during the HPLC purification. Normalized spectra of four additional elution peaks are shown in inset C. Their time-position in the HPLC profile are shown by arrows.

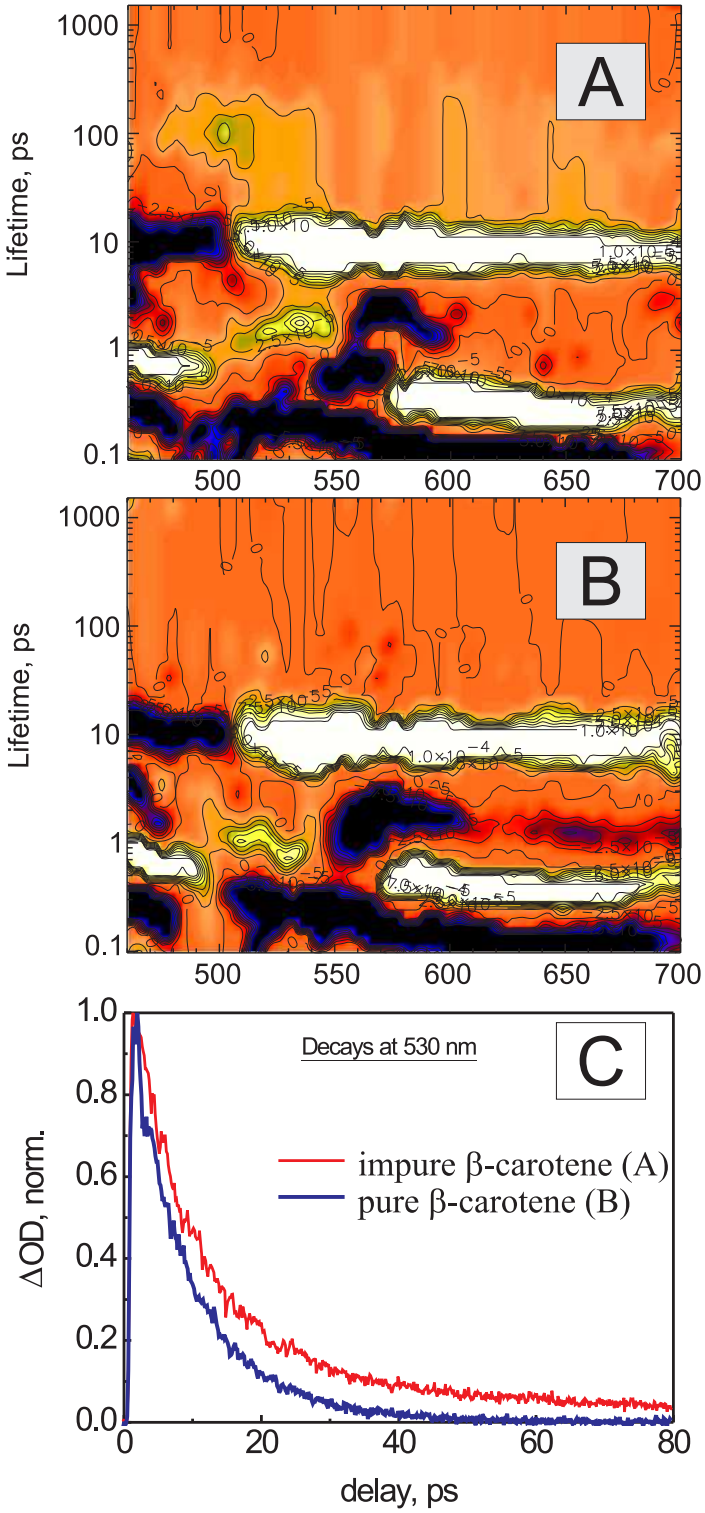


Figure S2. Lifetime density maps of β-carotene in MTHF before (A) and after (B) purification (corresponding to the HPLC profiles shown in Fig. S1A and B). Experimental TA decays measured at 530 nm in unpurified and purified samples (C). Excitation wavelength - 400 nm.

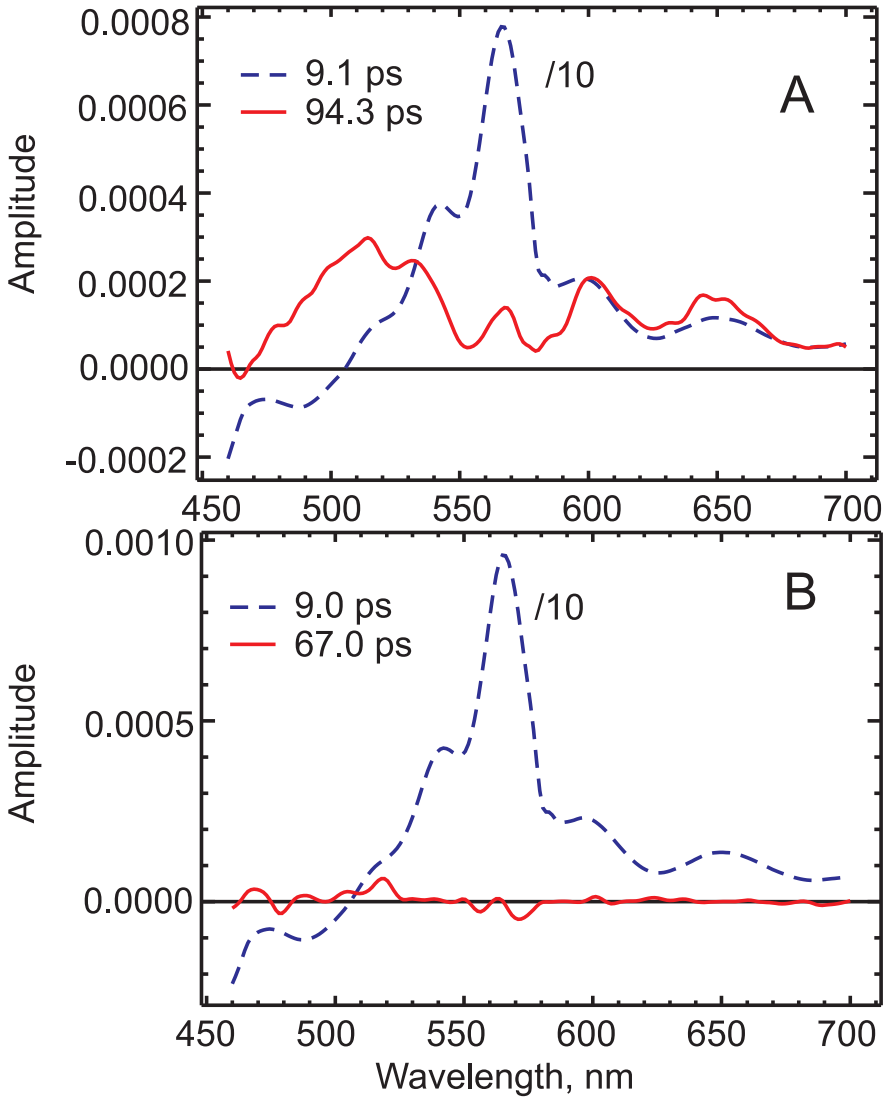


Figure S3. Global exponential analysis of data shown in Fig. S2 A and B, respectively. Analysis performed on the timescale >3 ps.

Table S1. Lifetimes τ of the hot-$S_0$, S* (or S*-reminiscent) and $S_1$ states reported in literature for various carotenoids of conjugation length N. $\lambda_{exc}$ – excitation wavelength, $I_{exc}$ – excitation intensity, n.d., not detected. Ref. – corresponding references.

| **Molecule** | **N** | **Solvent / Medium** | **$\lambda_{exc}$ (nm)** | **$I_{exc}$ per pulse / beam diameter** | **Photon density /cm$^2$/pulse** | **τ [ps], hot-$S_0$** | **τ [ps], S*/$S^{\ddagger}$/ $S_1$-trans** | **τ [ps], $S_1$** | **Ref.** |
|---|---|---|---|---|---|---|---|---|---|
| M15 | 15 | $CS_2$, toluene | 590 | 3 μJ / n.d. | n.d. | 6-13 | n.d. | 1-1.3 | 1 |
| M19 | 19 | hexane/ether/$CS_2$ | | | | 3-10 | | 0.4-0.6 | |
| Spirilloxanthin | 13 | hexane | 540 | <50 nJ / n.d. | n.d. | n.d. | 6 | 1.4 | 2 |
| Spheroidene | 10 | LH2 | 475 | 100 nJ / 150 μm | $1.4\times10^{14}$ | n.d. | 5 | 1.5 | 3 |
| Spirilloxanthin | 13 | hexane | 520 | 20 nJ / 200 μm | $1.7\times10^{14}$ | n.d. | n.d. | 1.35 | 4 |
| Spheroidene | 10 | reconstituted B850-complex | 500 | 50 nJ / 200 μm | $4\times10^{14}$ | n.d. | 7 | 1.5 | 5 |
| β-Carotene | 11 | hexane | 400, 500, 530 | 150 nJ / n.d. | n.d. | n.d. | 65 | 10 | 6 |
| β-Carotene | 11 | hexane | 490 | <70 nJ / 280 μm | $2.8\times10^{14}$ | 10.1 | n.d. | 9.3 | 7 |
| Zeaxanthin | 11 | methanol | | | | | | | |
| Lycopene | 11 | hexane | 505 | | | 5.8 | | 4.2 | |
| Zeaxanthin | 11 | methanol | 485 | 150 nJ / n.d. | n.d. | n.d. | n.d. | 9.2 | 8 |
| | | | 400 | | | | 2.8 | 9 | |
| | | | 266 | | | | 4.9 | 9.8 | |
| Neoxanthin | 8 | pyridine | 481 | 1 μJ / 1.2 mm | $2\times10^{14}$ | n.d. | 2.7 | 37.6 | 9 |
| Violaxanthin | 9 | | 485 | | | | 5 | 26.1 | |
| Lutein | 10 | | 491 | | | | 2.9 | 15.6 | |
| Zeaxanthin | 11 | | 497 | | | | 2.8 | 10.2 | |
| β-Carotene | 11 | | | | | | 3.4 | 9.5 | |
| Rhodopin glucosid | 11 | LH2 | 525 | 40-370 nJ / 200 μm | | n.d. | 30 | 3 | 10 |
| m9 | 9 | benzene | 450 | <80 nJ / n.d. | $4\times10^{14}$ | 39.1 | n.d. | 41.5 | 11 |
| β-Carotene | 11 | | 495 | | | 10.2 | | 9.5 | |

| | | | | | | | | | |
|---|---|---|---|---|---|---|---|---|---|
| M13 | 13 | | 525 | | | 6.7 | | 2.52 | |
| M15 | 15 | | 555 | | | 7.7 | | 1.02 | |
| Neurosporene | 9 | acetone + $CS_2$ (room T) | 0-0 transition | n.d. / n.d. | n.d. | n.d. | n.d. | 23 | 12 |
| Spheroidene | 10 | | | | | | 9.7 | 7.2 | |
| Rhodopin glucosid | 11 | | | | | | 5.2, 19 | 4.2 | |
| Rhodovibrin | 12 | | | | | | 3.1 | 2.2 | |
| Spirilloxanthin | 13 | | | | | | 3.8, 20 | 1.3 | |
| Neurosporene | 9 | 77K | | | | | n.d. | 35 | |
| Spheroidene | 10 | | | | | | n.d. | 11.6 | |
| Rhodopin glucosid | 11 | | | | | | 7.4 | 5.9 | |
| Rhodovibrin | 12 | | | | | | 8 | 2.7 | |
| Spirilloxanthin | 13 | | | | | | 3.8 | 1.7 | |
| Violaxanthin | 9 | EPA, 77K | 484 | 1 μJ / 1.2 mm | $2.2\times10^{14}$ | n.d. | n.d. | 33.5 | 13 |
| Lutein | 10 | | 491 | | | | 10.2 | 19.7 | |
| Zeaxanthin | 11 | | 500 | | | | 8.2 | 14.7 | |
| β-Carotene | 11 | Benzene / DMSO | 500 | n.d. / n.d. | $<10^{15}$ | n.d. | n.d. | 9.3/9/7 | 14 |
| Echinenone | 11 | | 500/515 | | | | n.d. | 6.2/6.4 | |
| Canthaxanthin | 13 | | 515/520 | | | | 9.1 | 4.5/4.9 | |
| Rhodoxanthin | 14 | | 545/550 | | | | 5.6/4 | 1.1/1.2 | |
| Neurosporene | 9 | EPA | 0-0 transition | n.d. / n.d. | n.d. | n.d. | 32 (trans) | n.d. | 15 |
| Spheroidene | 10 | | | | | | 12 (trans) | | |
| Spirilloxanthin | 13 | 2-MTHF | | | | | 4.9 (trans) | | |
| Neurosporene | 9 | EPA | 0-0 transition | | | | n.d. | 22 (cis) | |
| Spheroidene | 10 | | | | | | | 8.2 (cis) | |
| Spirilloxanthin | 13 | 2-MTHF | | | | | | 5.1 (cis) | |
| β-Carotene | 11 | benzonitrile | 545 | 8.5 nJ | $4\times10^{14}$ | n.d. | 10 | 9 | 16 |
| β-Carotene | 11 | 3-methyl-pentane | 400 | 50 nJ – 2 μJ / <200 μm | $3\times10^{14}$ – $1.7\times10^{16}$ | No detailed analysis provided | | | 17 |
| Rhodopin glucosid | 11 | LH2 | 525 | | | | | | |
| β-Carotene | 11 | n-hexane/acetone | 487/485 | 700 nJ / n.d. | $5\times10^{14}$ | 11.9 | n.d. | 8.7 | 18 |

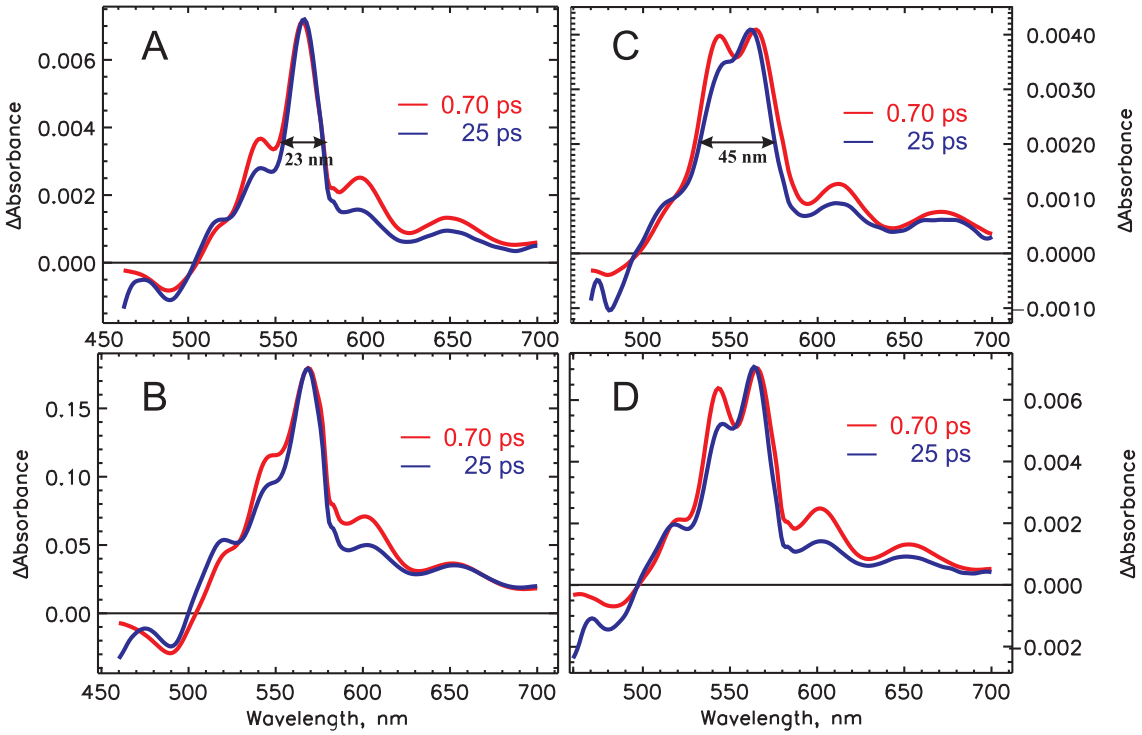


Figure S4. Normalised transient spectra of β-carotene for two delay times in MTHF (A-B) and n-hexane (C-D). Excitation intensity: 20 nJ (A), 1 μJ (B) and 14 nJ (C-D). Excitation wavelength: 400 nm (A-B, D) and 475 nm (C). The delay times were chosen to the values used in Chabera et al.[14] for comparison.

In Figure S4 a comparison of transient spectra taken at 0.7 ps and 25 ps delays is shown. Subfigures A-B represent intensity dependence, subfigures C-D represent excitation wavelength dependence. It follows that high intensity (Fig. S4B) and long wavelength excitation (Fig. S4C) leads to less resolved spectra and saturation of the maximum. As the result broadening and smoothing of the transient spectra can be observed, which at certain conditions can lead to very weak vibrational structure of the transient spectra, especially at longer delay times (blue lines in Fig. S4). The narrowing of the bleaching in the ≤500 nm region is observed at longer delay time in agreement with Chabera et al.[14]. One of the possible reasons of such behavior might be higher ground state homogeneity at longer delay times [14,19]. However it can also not be excluded that this effect is actually caused by changes in the $S_1$ ESA spectra at different delay times.

**Table S2.** Values of spectral width of the $S_1$-$S_{1N}$ ESA peak at half maximum (FWHM) of β-carotene in selected references.

| Reference | Niedzwiedzki et al. [9] | Chabera et al. [14] | Buckup et al. [11] | De Weerd et al. [20] | this work |
|---|---|---|---|---|---|
| Fig. / page | Fig. 5A, p.22876 | Fig. 3 top, p.8798 | Fig. 3A, p.194505-5 | Fig. 2A/C , p.40 | Fig. S4, SI |
| $S_1$-$S_{1N}$ peak width / solvent | 59 nm / pyridine | 55 nm / benzene | 45 nm / benzene | 41 nm / hexane<br>51 nm / benzyl alcohol | 23 nm / MTHF<br>45 nm / hexane |

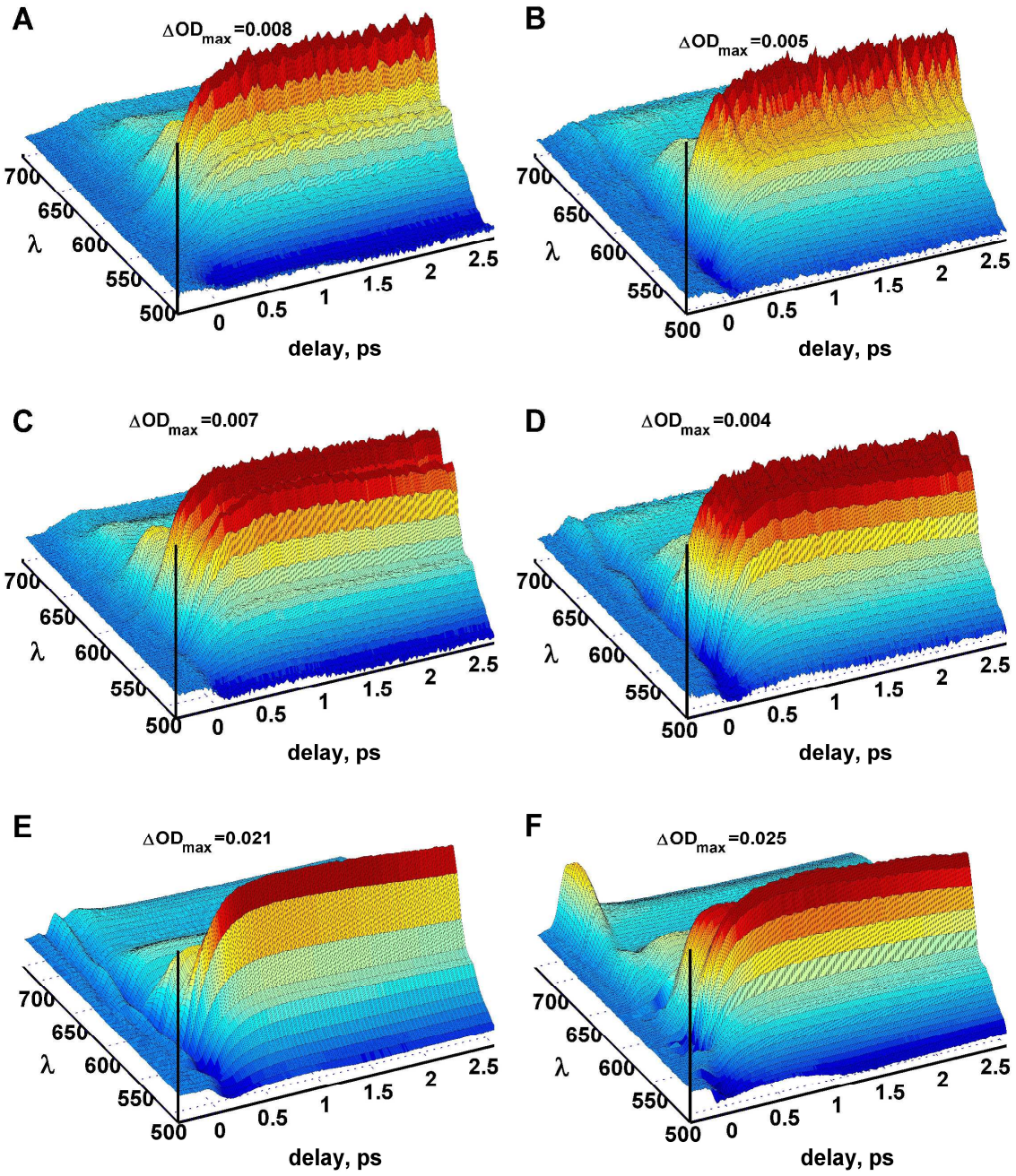


Figure S5. Original 3D data sets (*ΔOD* vs. time and wavelength) of the TA signals of β-carotene in MTHF excited at 400 nm (A) and 485 nm (B), in n-hexane excited at 400 nm (C), 475 nm (D), 485 nm (E), and 509 nm (F). For convenience of presentation transient data are normalized to the maximum, the maximal optical density is shown for each measurement.

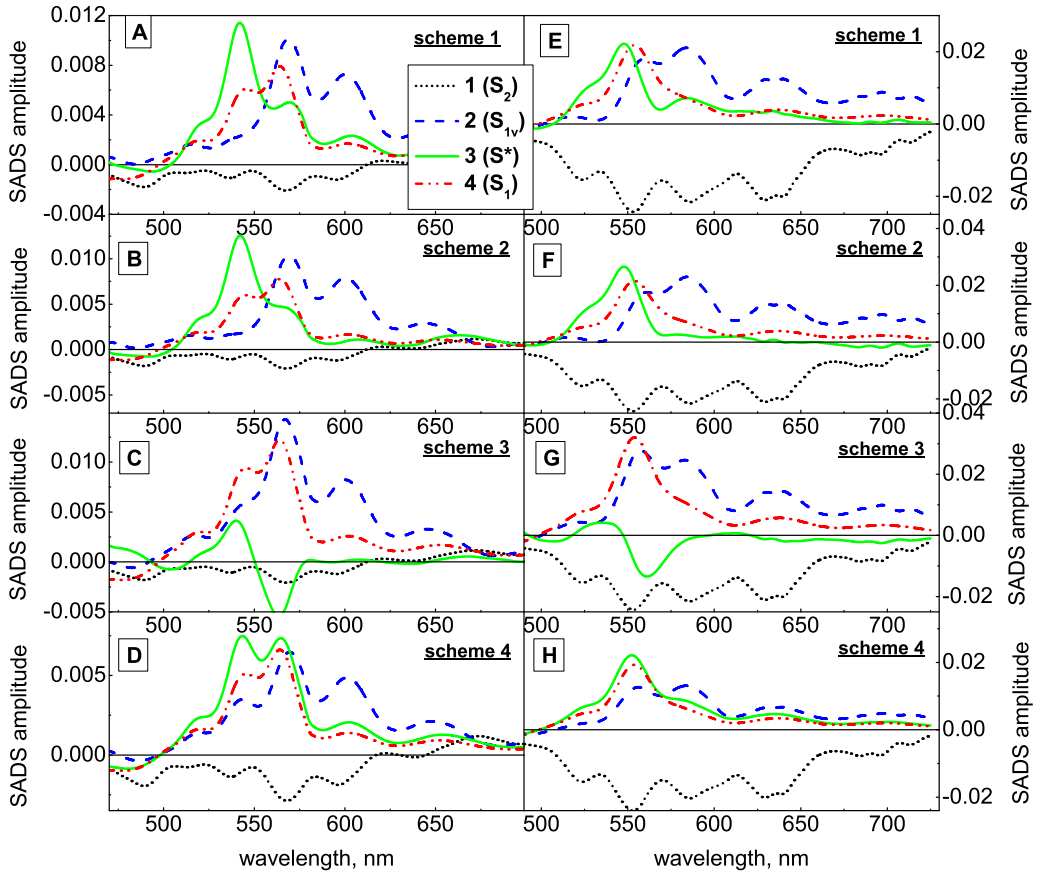


Figure S6. Resulting SADS for target analysis of the TA signals for β-carotene in hexane excited at 400 nm (A-D) and 485 nm (E-H). The different SADS correspond to target analyses using the kinetic schemes shown in Fig. 4.

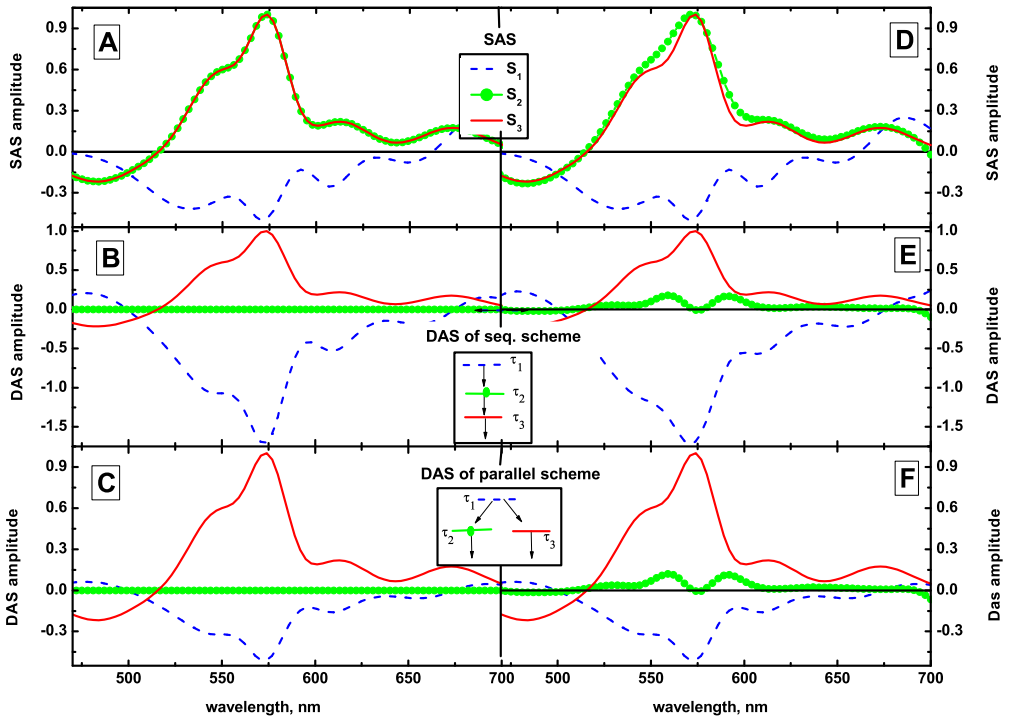


Figure S7. Simulated DADS (B-C and E-F) calculated from the assumed SADS (A and D) in the case of a sequential (B and E) and a parallel (C and F) kinetic scheme. Note that in panels A-C the 2nd and 3rd SADS are identical, resulting in a zero DADS for component 2, in panels D-F the 2nd and 3rd SAS differ slightly, resulting in a non-zero DADS of low overall amplitude.

## SADS vs. DADS and EADS

Decay-associated spectra (DADS) and the corresponding lifetime result from sums of exponentials lifetime analysis of the original data and can be performed entirely independent from any available information on the underlying kinetic models[21,22]. The results are pure mathematical parameters that do not provide any information on the underlying physical model(s). This kind of (often global) analysis can be performed on any set of data and allows to exclude models that are too simple to explain the data and gives a hint on the minimal complexity (number of components) a kinetic model must have in order to satisfy mathematically the observed kinetics.

In case that the underlying kinetic model is known, the lifetimes represent the inverse of the eigenvalues of the relevant kinetic matrix of the system, and the DADS represent linear combinations of the true species-associated spectra (SADS), which are the initial excitation condition weighted eigenvectors of the system[21,22]. For these reasons DADS are not suitable for a detailed analysis of spectra of intermediates, since without the knowledge of the underlying kinetic scheme DADS and in particular also their relative amplitudes and spectral forms can not be interpreted in a meaningful way.

They merely show that a certain number of independent kinetic components (corresponding to the different lifetimes) is present in the data. The global lifetime analysis resulting in DADS and the corresponding lifetimes is a very common way of performing a first analysis of time-resolved data at a stage when generally no further information on the kinetics and intermediates of a system is available. Notably often also so-called evolution-associated spectra (EADS) and related rates (inverse lifetimes) are calculated corresponding to a sequential reaction scheme[22]. Such EADS do not provide any specific or additional information or advantage over DADS however, unless the true underlying kinetic scheme of the system is really sequential. In the latter case the EADS become identical to the true SADS. In all other cases the EADS also represent complicated linear combinations of the true SADS – however different from DADS. Therefore the detailed spectral forms and (relative) amplitudes of EADS can not be discussed or understood in a meaningful manner in all but the simplest cases as well. We note that in the literature on carotenoid TA measurements often DADS and/or EADS have been used to discuss their spectral shapes or differences in their spectral shapes in order to elucidate the molecular nature and origin of the corresponding intermediates. However such a discussion is in most cases not meaningful and can easily lead to unjustified conclusions.

For a chemical/physical system the real physical parameters of interest in general are the rate constants of the kinetic scheme of the system (described by a kinetic matrix) and the corresponding SADS, which are the actual (difference) spectra of the intermediates of the system. The simulations in Fig. S7 demonstrate that the DADS amplitude of a kinetic component can be small, or even zero, in spite of the respective intermediate having a very similar – or even identical – spectrum as another component. This is exactly the case for some components observed in the TA relaxation kinetics of carotenoids and requires caution.

Typically, the underlying kinetic scheme of a system is not known *a priori*. Rather the task is to determine that scheme based on the kinetic data. This can only be done in general by comparing the resulting SADS (and rate constants) from (global) target analysis on different kinetic schemes applied to the same data set. Very often the formal fit criteria ($\chi^2$-values, residual plots etc.) are identical and very good for several different kinetic models and can thus not be used to distinguish between them[21,22]. The results must then be judged based on additional knowledge allowing to determine which rates and spectra are “physically reasonable” and which ones are not. In many cases it is possible to exclude certain kinetic schemes because they provide physically unreasonable results (SADS and/or rates). It may well happen however that not all the

potentially possible kinetic schemes can be distinguished. In such cases additional and complementary experiments (using other detection methods etc.) providing additional information are required, which then often allows to distinguish such models. The important point for the present paper is that a meaningful analysis, discussion, and judgment of the spectral forms of the intermediates can only be performed on the basis of the SADS but not on the basis of DADS or EADS.

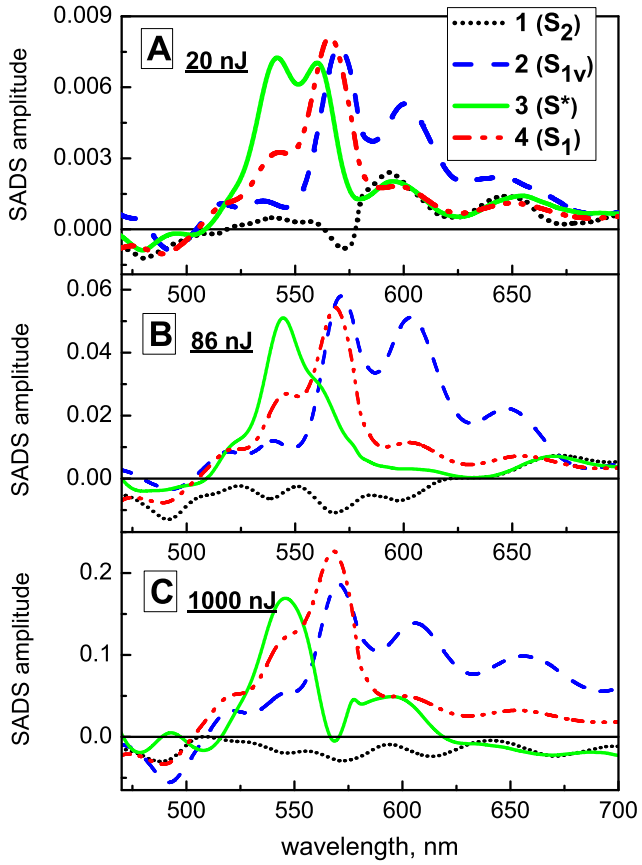


Figure S8. SADS resulting from target analysis of the TA signals of β-carotene in MTHF excited at 400 nm with 20 nJ pulses (A), 86 nJ pulses (B) and 1 μJ pulses (C). The SADS correspond to target analysis using kinetic scheme 2 in Fig.4.

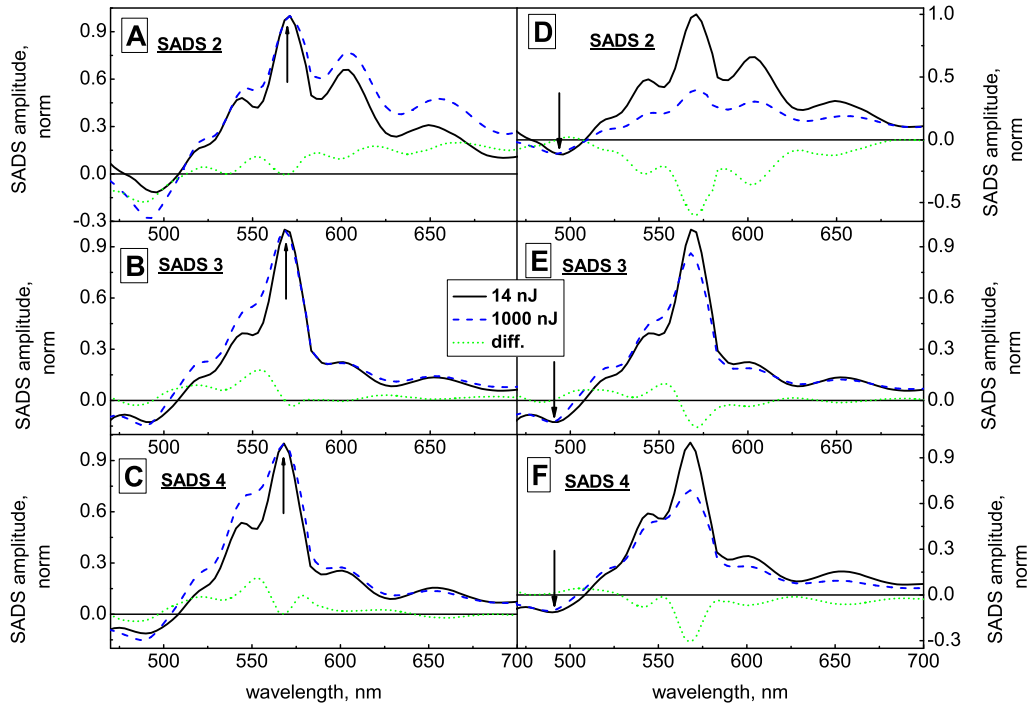


Figure S9. Comparison of 2nd (A and D), 3rd (B and E) and 4th (C and F) SADS from low intensity (14 nJ, black solid line) and high intensity (1 μJ, blue dashed line) measurements of β-carotene in hexane. The difference spectrum is shown by the green dotted line. For analysis the sequential kinetic scheme 4 was used. SADS are normalized either to the maximum (A-C), or to the GB signal (D-F) (shown by the arrow).

## References


1. Andersson, P. O.; Gillbro, T. Photophysics and dynamics of the lowest excited singlet state in long substituted polyenes with implications to the very long-chain limit. *J. Chem. Phys.* **1995,** *103*, 2509-2519.

2. Gradinaru, C. C.; Kennis, J. T. M.; Papagiannakis, E.; van Stokkum, I. H. M.; Cogdell, R. J.; Fleming, G. R.; Niederman, R. A.; van Grondelle, R. An unusual pathway of excitation energy deactivation in carotenoids: Singlet-to-triplet conversion on an ultrafast timescale in a photosynthetic antenna. *Proc. Natl. Acad. Sci. USA* **2001,** *98* (5), 2364-2369.

3. Papagiannakis, E.; Kennis, J. T. M.; van Stokkum, I. H. M.; Cogdell, R. J.; van Grondelle, R. An alternative carotenoid-to-bacteriochlorophyll energy transfer pathway in photosynthetic light harvesting. *Proc. Natl. Acad. Sci. USA* **2002,** *99* (9), 6017-6022.

4. Papagiannakis, E.; van Stokkum, I. H. M.; van Grondelle, R.; Niederman, R. A.; Zigmantas, D.; Sundström, V.; Polivka, T. A near-infrared transient absorption study of the excited-state dynamics of the carotenoid spirilloxanthin in solution and in the LH1 complex of *Rhodospirillum rubrum*. *J. Phys. Chem. B* **2003,** *107* (40), 11216-11223.

5. Papagiannakis, E.; Das, S. K.; Gall, A.; van Stokkum, I. H. M.; Robert, B.; van Grondelle, R.; Frank, H. A.; Kennis, J. T. M. Light harvesting by carotenoids incorporated into the B850 light-harvesting complex from *Rhodobacter sphaeroides* R-26.1: Excited-state relaxation, ultrafast triplet formation, and energy transfer to bacteriochlorophyll. *J. Phys. Chem. B* **2003,** *107* (23), 5642-5649.

6. Larsen, D. S.; Papagiannakis, E.; van Stokkum, I. H. M.; Vengris, M.; Kennis, J. T. M.; van Grondelle, R. Excited state dynamics of β-carotene explored with dispersed multi-pulse transient absorption. *Chem. Phys. Lett.* **2003,** *381* (5-6), 733-742.

7. Wohlleben, W.; Buckup, T.; Hashimoto, H.; Cogdell, R. J.; Herek, J. L.; Motzkus, M. Pump-deplete-probe spectroscopy and the puzzle of carotenoid dark states. *J. Phys. Chem. B* **2004,** *108* (10), 3320-3325.

8. Billsten, H. H.; Pan, J.; Sinha, S.; Pascher, T.; Sundström, V.; Polivka, T. Excited-state processes in the carotenoid zeaxanthin after excess energy excitation. *J. Phys. Chem. A* **2005,** *109* (31), 6852-6859.

9. Niedzwiedzki, D. M.; Sullivan, J. O.; Polivka, T.; Birge, R. R.; Frank, H. A. Femtosecond time-resolved transient absorption spectroscopy of xanthophylls. *J. Phys. Chem. B* **2006,** *110* (45), 22872-22885.

10. Papagiannakis, E.; van Stokkum, I. H. M.; Vengris, M.; Cogdell, R. J.; van Grondelle, R.; Larsen, D. S. Excited-state dynamics of carotenoids in light-harvesting complexes. 1. Exploring the relationship between the $S_1$ and S* states. *J. Phys. Chem. B* **2006,** *110* (11), 5727-5736.

11. Buckup, T.; Savolainen, J.; Wohlleben, W.; Herek, J. L.; Hashimoto, H.; Correia, R. R. B.; Motzkus, M. Pump-probe and pump-deplete-probe spectroscopies on carotenoids with N=9-15 conjugated bonds. *J. Chem. Phys.* **2006,** *125* (19), 194505-1-194505-7.

12. Niedzwiedzki, D.; Koscielecki, J. F.; Cong, H.; Sullivan, J. O.; Gibson, G. N.; Birge, R. R.; Frank, H. A. Ultrafast dynamics and excited state spectra of open-chain carotenoids at room and low temperatures. *J. Phys. Chem. B* **2007,** *111* (21), 5984-5998.

13. Cong, H.; Niedzwiedzki, D. M.; Gibson, G. N.; Frank, H. A. Ultrafast time-resolved spectroscopy of xanthophylls at low temperature. *J. Phys. Chem. B* **2008,** *112* (11), 3558-3567.

14. Chabera, P.; Fuciman, M.; Hribek, P.; Polivka, T. Effect of carotenoid structure on excited-state dynamics of carbonyl carotenoids. *Phys. Chem. Chem. Phys.* **2009,** *11*, 8795-8803.

15. Niedzwiedzki, D. M.; Sandberg, D. J.; Cong, H.; Sandberg, M. N.; Gibson, G. N.; Birge, R. R.; Frank, H. A. Ultrafast time-resolved absorption spectroscopy of geometric isomers of carotenoids. *Chemical Physics* **2009,** *357*, 4-16.

16. Christensson, N.; Milota, F.; Nemeth, A.; Sperling, J.; Kauffmann, H. F.; Pullerits, T.; Hauer, J. Two-dimensional electronic spectroscopy of $\beta$-carotene. *J. Phys. Chem. B* **2009,** *113*, 16409-16419.

17. Jailaubekov, A. E.; Song, S. H.; Vengris, M.; Cogdell, R. J.; Larsen, D. S. Using narrowband excitation to confirm that the S* state in carotenoids is not a vibrationally-excited ground state species. *Chem. Phys. Lett.* **2010,** *487* (1-3), 101-107.

18. Lenzer, T.; Ehlers, F.; Scholz, M.; Oswald, R.; Oum, K. Assignment of carotene S* state features to the vibrationally hot ground electronic state. *Phys. Chem. Chem. Phys.* **2010,** *12*, 8832-8839.

19. Christensen, R. L.; Galinato, M. G. I.; Chu, E. F.; Fujii, R.; Hashimoto, H.; Frank, H. A. Symmetry control of radiative decay in linear polyenes: Low barriers for isomerization in the S-1 state of hexadecaheptaene. *J. Am. Chem. Soc.* **2007,** *129*, 1769-1775.

20. de Weerd, F. L.; van Stokkum, I. H. M.; van Grondelle, R. Subpicosecond dynamics in the excited state absorption of all- *trans*-β-Carotene. *Chem. Phys. Lett.* **2002,** *354* (1-2), 38-43.

21. Holzwarth, A. R. Data analysis of time-resolved measurements. In *Biophysical Techniques in Photosynthesis. Advances in Photosynthesis Research*, Amesz, J., Hoff, A. J., Eds.; Kluwer Academic Publishers: Dordrecht, 1996; pp 75-92.

22. van Stokkum, I. H. M.; Larsen, D. S.; van Grondelle, R. Global and target analysis of time-resolved spectra. *Biochim. Biophys. Acta* **2004,** *1657* (2-3), 82-104.